Available online at www.sciencedirect.com
ScienceDirect
Journal of Sound and Vibration 305 (2007) 728–749
JOURNAL OF SOUND AND VIBRATION
www.elsevier.com/locate/jsvi

Dynamic modeling of active constrained layer damping of composite beam under thermal environment

Sharnappa, N. Ganesan*, Raju Sethuraman

Department of Mechanical Engineering, Indian Institute of Technology Madras, Chennai 600 036, India

Received 20 January 2006; received in revised form 28 July 2006; accepted 21 April 2007
Available online 8 June 2007

Abstract

The present work deals with the active vibration control of composite beam under thermal environment using finite element method. The effect of fiber orientation and temperature on natural frequency and damping of the system are investigated for different boundary conditions. The temperature-dependent properties of viscoelastic core are considered. Results are presented for frequencies and loss factor with different core material and core thickness. Characteristics of loss factor and frequency near the buckling temperature are discussed, and the effect of core thickness on buckling temperature is also investigated.

1. Introduction

Among the various types of damping treatments active constrained layer damping (ACLD) treatment is found to be more effective for the structural members, which judiciously combines the advantages of both the passive and active damping treatments. ACLD treatments applied to composite beams are very rare in open literature. Ray and Reddy [1,2] presented the active control of the vibration of laminated circular cylindrical composite shells have been demonstrated using optimally placed patches of ACLD treatment. They also investigated the analysis of ACLD of laminated thin composite shells using piezoelectric fiber-reinforced composite (PFRC) materials. Ray and Mallik [3,4] have theoretically investigated the effectiveness of PFRC material in the development of new actuators as smart structures. They have also extended the study to the plate-type structures. Ray and Baz [5] have optimized the energy dissipation characteristics of ACLD treatments of plates using rational design procedure. Ray et al. [6] presented the effectiveness of the ACLD treatments in enhancing the damping characteristics of thin cylindrical shells. A finite element model is developed to describe the dynamic interaction between the shells and the ACLD treatments. Chantalakhana and Stanway [7] conducted the experiment and numerical study of the application of ACLD to a clamped–clamped plate.

Sung and Kam [8] investigated on composite beams treated with active constraining layer. Sun and Huang [9] studied the vibration suppression of laminated composite beams with a piezo-electric damping layer.

*Corresponding author.
E-mail address: nganesan@iitm.ac.in (N. Ganesan).

0022-460X/$ - see front matter © 2007 Elsevier Ltd. All rights reserved.
doi:10.1016/j.jsv.2007.04.033

Khatua and Cheung [10] presented the formulation of for bending and vibration of multiplayer beams and plates with constrained cores. Gaudenzi et al. [11] investigated the vibration control of an active laminated beam. Balamurugan and Narayanan [12] presented a finite element formulation and active vibration control of isotropic beams with smart constrained layer damping. Hau and Fung [13] studied the effect of ACLD treatment configuration on damping performance of a flexible beam. Pradeep and Ganesan [14] presented the vibration behavior of ACLD treated isotropic beams under thermal environment.

Literature on ACLD composite beam under thermal environment, considering thermally induced pre-stresses and temperature-dependent shear modulus of the core is not reported. The present work deals with vibration study of an ACLD composite beam subjected to a tip temperature with different boundary conditions using Finite Element Method (FEM). The loss factor and natural frequency variation with respect to temperature considering the temperature-dependent material loss factor of the core are reported. The loss factor and frequency variation with respect to fiber orientation also studied. In addition, the relative influence of a structural damping of composite material, passive damping of viscoelastic material and active damping is analyzed.

2. Finite element formulation

A finite element model has been developed to describe the dynamic behavior of a composite beam with ACLD treatment under thermal environment. Thermally induced pre-stresses are calculated for the composite beam. The two noded elements are used to evaluate the temperature field in the beam. For this purpose to start with Fourier heat conduction equation is used to evaluate temperatures in the beam. The sandwich beam element is developed based on the displacement field proposed by Khatua and Cheung [10] (refer to Fig. 1).

The sensor is rigidly bounded to the composite beam and viscoelastic layer (VEL) is placed in between the sensor and actuator. The actuator, sensor and composite beam act as stiff layer, the configuration of the FEM model with degree of freedom per node is shown in Fig. 1. In the present study the base beam is made of Graphite/Epoxy composite material. The geometry of the beam used is similar to Hau and Fung [13] and the material properties for the present study are referred from Refs. [13,15,16] which are given in Table 1.

The following assumptions are made in deriving the finite element model:

1. The sensor layer is perfectly bounded to the base beam.
2. The combined base beam and sensor layer behave like an equivalent single layer.
3. The transverse shear in the stiff layers is neglected.
4. The core material is viscoelastic with temperature-dependent complex shear modulus [16]

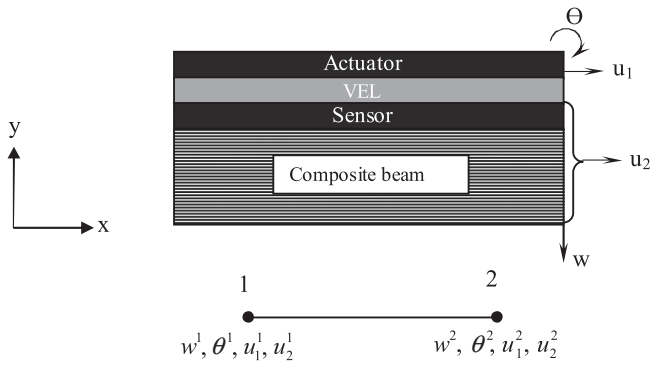

Fig. 1. Composite beam with hybrid damping treatment.

Table 1
System parameters

	Geometry (m)	Properties
Piezoelectric layer	$L = 0.2616$ $b = 0.0127$ $t = 0.000762$	$\rho = 7600\,\mathrm{kg/m^3}$, $E = 6.49 \times 10^{10}\,\mathrm{N/m^2}$ $d_{31} = -1.75 \times 10^{-10}\,\mathrm{m/V}$ $e_{13} = 5.2\,\mathrm{N/Vm}$ $\varepsilon_{33} = 1.5 \times 10^{-8}\,\mathrm{F/m}$
Core	$L = 0.2616$ $b = 0.0127$ $t_c = 0.00025$	$G^*_{(T=30\,^\circ\mathrm{C})} = 0.187(1+0.388\mathrm{i})$ GPa (DYAD606) $\rho_c = 1200\,\mathrm{kg/m^3}$ (DYAD606) $G^*_{(T=30\,^\circ\mathrm{C})} = 0.575(1+0.3\mathrm{i})$ GPa (EC2216) $\rho_c = 1250\,\mathrm{kg/m^3}$ (EC2216)
Base beam	$L = 0.2616$ $b = 0.0127$ $t_b = 0.002286$	$K_x = 4.62\,\mathrm{W/mK}$, $K_y = 0.72\,\mathrm{W/mK}$ $E_{11} = 137.8\,\mathrm{GPa}$, $E_{22} = 8.96\,\mathrm{GPa}$, $G_{12} = 7.1\,\mathrm{GPa}$ $\rho_b = 1600\,\mathrm{kg/m^3}$, $v_{12} = 0.3$ $\eta_{11} = 0.0045$, $\eta_{22} = 0.0422$, $\eta_{12} = 0.075$ $\alpha_{11} = -0.3 \times 10^{-6}\,\mathrm{K^{-1}}$, $\alpha_{22} = 26.08 \times 10^{-6}\,\mathrm{K^{-1}}$

The composite beam treated with ACLD along with four degrees of freedom per node (w,θ,u_1,u_2) used for the modeling of the beam as shown in Fig. 1. The equation of motion for the sandwich composite beam under thermal environment can be written as

$$[M]\{\ddot{\delta}_G\} + [C]\{\dot{\delta}_G\} + [[K] + [K_g]]\{\delta_G\} = 0, \tag{1}$$

where $[M]$, $[C]$, $[K]$, $[K_g]$, $\{\delta_G\}$ are the mass matrix, piezo electric damping matrix, complex stiffness matrix resulting due to viscoelastic core, geometric stiffness matrix and displacement vector, respectively. The expressions for stiffness matrix, mass matrix and geometric stiffness matrix are similar to the formulation presented in Refs. [10,17,18] except that the composite layers have to be accounted with the relevant constitutive matrix. Details of derivation of above matrixes at elemental level are described in the subsequent sections.

2.1. Stiffness matrix and thermal load vector

The stress–strain relations are written in the form of stress and moment resultants for composite laminates which are given in Refs. [18]. These stress and moment resultants are reduced to a beam which are used for the formulation as follows.

The stress–strain relations for a generally orthotropic lamina are given by

$$\begin{Bmatrix} \sigma_{xx} \\ \sigma_{yy} \\ \sigma_{xy} \end{Bmatrix} = \begin{bmatrix} \overline{Q}_{11} & \overline{Q}_{11} & \overline{Q}_{11} \\ \overline{Q}_{11} & \overline{Q}_{11} & \overline{Q}_{11} \\ \overline{Q}_{11} & \overline{Q}_{11} & \overline{Q}_{11} \end{bmatrix} \begin{Bmatrix} \varepsilon_{xx} - \alpha_{xx}(\Delta T) \\ \varepsilon_{yy} - \alpha_{yy}(\Delta T) \\ \varepsilon_{xy} - \alpha_{xy}(\Delta T) \end{Bmatrix}, \tag{2}$$

where α_{xx}, α_{yy} and α_{xy} are thermal expansion coefficients in the principal directions. ΔT is the temperature rise and $\overline{Q_{ij}}$ are plane stress-reduced stiffness coefficients.

From Eq. (2), the stress and moment resultants are obtained by the integration of stresses over the thickness 'h' of the stiff layer:

$$\begin{bmatrix} N_{xx} \\ N_{yy} \\ N_{xy} \end{bmatrix} = \int_{-h/2}^{h/2} \begin{bmatrix} \sigma_{xx} \\ \sigma_{yy} \\ \sigma_{xy} \end{bmatrix} \mathrm{d}z \quad \begin{bmatrix} M_{xx} \\ M_{yy} \\ M_{xy} \end{bmatrix} = \int_{-h/2}^{h/2} \begin{bmatrix} \sigma_{xx} \\ \sigma_{yy} \\ \sigma_{xy} \end{bmatrix} z\,\mathrm{d}z. \tag{3}$$

Eq. (3) can be written as

$$\begin{Bmatrix} N_{xx} \\ N_{yy} \\ N_{xy} \\ M_{xx} \\ M_{yy} \\ M_{xy} \end{Bmatrix} = \begin{bmatrix} A_{11} & A_{12} & A_{13} & B_{11} & B_{12} & B_{13} \\ A_{21} & A_{22} & A_{23} & B_{21} & B_{22} & B_{23} \\ A_{31} & A_{32} & A_{33} & B_{31} & B_{32} & B_{33} \\ B_{11} & B_{12} & B_{13} & D_{11} & D_{12} & D_{13} \\ B_{21} & B_{22} & B_{23} & D_{21} & D_{22} & D_{23} \\ B_{31} & B_{32} & B_{33} & D_{31} & D_{32} & D_{33} \end{bmatrix} \begin{Bmatrix} \varepsilon^0_{xx} \\ \varepsilon^0_{yy} \\ \varepsilon^0_{xy} \\ k_{xx} \\ k_{yy} \\ k_{xy} \end{Bmatrix} - \begin{Bmatrix} N_{txx} \\ N_{tyy} \\ N_{txy} \\ M_{txx} \\ M_{tyy} \\ M_{txy} \end{Bmatrix}, \tag{4}$$

where A_{ij}, B_{ij} and D_{ij} are extensional stiffness, flexural–extensional coupling stiffness and flexural stiffness, respectively. These are expressed as follows:

$$\left(A_{ij}B_{ij}D_{ij}\right) = \sum_{m=1}^{nlay} \int_{z_m}^{z_{m+1}} \overline{Q}^m_{ij}\left(1, Z, Z^2\right) \mathrm{d}z, \quad i,j = 1,2,3, \tag{5}$$

$\overline{Q^m_{ij}}$ is the reduced stiffness coefficients of the mth layer with ply thickness z_m to z_{m+1}.

The thermal stress resultants $[N_t]$ and moment resultants $[M_t]$ are defined as

$$[N_t] = \begin{bmatrix} N_{txx} \\ N_{tyy} \\ N_{txy} \end{bmatrix} = \sum_{m=1}^{nlay} \int_{z_m}^{z_{m+1}} \overline{Q^m_{ij}} \begin{bmatrix} \alpha_{xx} \\ \alpha_{yy} \\ 2\alpha_{xy} \end{bmatrix} (\Delta T)\, \mathrm{d}z \quad i,j = 1,2,3, \tag{6}$$

$$[M_t] = \begin{bmatrix} M_{txx} \\ M_{tyy} \\ M_{txy} \end{bmatrix} = \sum_{m=1}^{nlay} \int_{z_m}^{z_{m+1}} \overline{Q^m_{ij}} \begin{bmatrix} \alpha_{xx} \\ \alpha_{yy} \\ 2\alpha_{xy} \end{bmatrix} (\Delta T) z\, \mathrm{d}z \quad i,j = 1,2,3. \tag{7}$$

Eq. (4) can be rewritten into two Eqs. (8) and (9) as follows:

$$\begin{Bmatrix} N_{xx} \\ M_{xx} \end{Bmatrix} = \begin{bmatrix} A_{11} & B_{11} \\ B_{11} & D_{11} \end{bmatrix} \begin{Bmatrix} \varepsilon^0_{xx} \\ k_{xx} \end{Bmatrix} + \begin{bmatrix} A_{12} & A_{13} & B_{12} & B_{13} \\ B_{12} & B_{13} & D_{12} & D_{13} \end{bmatrix} \begin{Bmatrix} \varepsilon^0_{yy} \\ \varepsilon^0_{xy} \\ k_{yy} \\ k_{xy} \end{Bmatrix} - \begin{Bmatrix} N_{txx} \\ M_{txx} \end{Bmatrix}, \tag{8}$$

$$\begin{bmatrix} A_{21} & B_{21} \\ A_{31} & B_{31} \\ B_{21} & D_{21} \\ B_{31} & D_{31} \end{bmatrix} \begin{Bmatrix} \varepsilon^0_{xx} \\ k_{xx} \end{Bmatrix} + \begin{bmatrix} A_{22} & A_{23} & B_{22} & B_{23} \\ A_{32} & A_{33} & B_{32} & B_{33} \\ B_{22} & B_{23} & D_{22} & D_{23} \\ B_{32} & B_{33} & D_{32} & D_{33} \end{bmatrix} \begin{Bmatrix} \varepsilon^0_{yy} \\ \varepsilon^0_{xy} \\ k_{yy} \\ k_{xy} \end{Bmatrix} - \begin{Bmatrix} N_{tyy} \\ N_{txy} \\ M_{tyy} \\ M_{txy} \end{Bmatrix} = \begin{Bmatrix} N_{yy} \\ N_{xy} \\ M_{yy} \\ M_{xy} \end{Bmatrix}. \tag{9}$$

Since in case of a beam there are no stress and moment resultants in y–y and x–y directions because a beam is one-dimensional, so in the above equation

$$N_{yy} = N_{xy} = M_{yy} = M_{xy} = 0.$$

After applying the assumptions of the beam, Eq. (9) can be written as

$$\begin{Bmatrix} \varepsilon^0_{yy} \\ \varepsilon^0_{xy} \\ k_{yy} \\ k_{xy} \end{Bmatrix} = \begin{bmatrix} A_{22} & A_{23} & B_{22} & B_{23} \\ A_{32} & A_{33} & B_{32} & B_{33} \\ B_{22} & B_{23} & D_{22} & D_{23} \\ B_{32} & B_{33} & D_{32} & D_{33} \end{bmatrix}^{-1} \left(\begin{Bmatrix} N_{tyy} \\ N_{txy} \\ M_{tyy} \\ M_{txy} \end{Bmatrix} - \begin{bmatrix} A_{21} & B_{21} \\ A_{31} & B_{31} \\ B_{21} & D_{21} \\ B_{31} & D_{31} \end{bmatrix} \begin{Bmatrix} \varepsilon^0_{xx} \\ k_{xx} \end{Bmatrix} \right). \tag{10}$$

Substituting the value of $\left\{\varepsilon_{yy}^0\ \varepsilon_{xy}^0\ k_{yy}\ k_{xy}\right\}^{\mathrm{T}}$ from Eq. (10) into Eq. (8) and after simplification leads to the following equation:

$$\begin{Bmatrix} N_{xx} \\ M_{xx} \end{Bmatrix} = \begin{bmatrix} A_{11}^* & B_{11}^* \\ B_{11}^* & D_{11}^* \end{bmatrix} \begin{Bmatrix} \varepsilon_{xx}^0 \\ k_{xx} \end{Bmatrix} - \begin{Bmatrix} N_{txx}^* \\ M_{txx}^* \end{Bmatrix}, \tag{11}$$

where

$$\begin{bmatrix} A_{11}^* & B_{11}^* \\ B_{11}^* & D_{11}^* \end{bmatrix} = \begin{bmatrix} A_{11} & B_{11} \\ B_{11} & D_{11} \end{bmatrix} - \begin{bmatrix} A_{12} & A_{13} & B_{12} & B_{13} \\ B_{12} & B_{13} & D_{12} & D_{13} \end{bmatrix} \left(\begin{bmatrix} A_{22} & A_{23} & B_{22} & B_{23} \\ A_{32} & A_{33} & B_{32} & B_{33} \\ B_{22} & B_{23} & D_{22} & D_{23} \\ B_{32} & B_{33} & D_{32} & D_{33} \end{bmatrix}^{-1} \begin{bmatrix} A_{21} & B_{21} \\ A_{31} & B_{31} \\ B_{21} & D_{21} \\ B_{31} & D_{31} \end{bmatrix} \right),$$

$$\begin{bmatrix} N_{txx}^* \\ M_{txx}^* \end{bmatrix} = \begin{bmatrix} A_{12} & A_{13} & B_{12} & B_{13} \\ B_{12} & B_{13} & D_{12} & D_{13} \end{bmatrix} \left(\begin{bmatrix} A_{22} & A_{23} & B_{22} & B_{23} \\ A_{32} & A_{33} & B_{32} & B_{33} \\ B_{22} & B_{23} & D_{22} & D_{23} \\ B_{32} & B_{33} & D_{32} & D_{33} \end{bmatrix}^{-1} \begin{Bmatrix} N_{tyy} \\ N_{txy} \\ M_{tyy} \\ M_{txy} \end{Bmatrix} \right) - \begin{Bmatrix} N_{txx} \\ M_{txx} \end{Bmatrix}.$$

Eq. (11) can be written as follows:

$$\{E\} = [D^*]_{si}\{\varepsilon\}_{si} - \left[D_1^*\right]_{si}, \tag{12}$$

where $i = 1$ for top stiff layer and 2 for bottom stiff layer

$$\{E\} = \begin{Bmatrix} N_{xx} \\ M_{xx} \end{Bmatrix}; \quad [D^*] = \begin{bmatrix} A_{11}^* & B_{11}^* \\ B_{11}^* & D_{11}^* \end{bmatrix}; \quad \{\varepsilon\} = \begin{Bmatrix} \varepsilon_{xx}^0 \\ k_{xx} \end{Bmatrix}; \quad \left[D_1^*\right] = \begin{Bmatrix} N_{txx}^* \\ M_{txx}^* \end{Bmatrix}.$$

The total potential of a composite sandwich beam under thermal load is given by

$$U = U_m + U_t, \tag{13}$$

where U_m and U_t are the potential due to mechanical and thermal effects, respectively, which are expressed as follows:

$$U_m = \frac{1}{2} b \int_0^l \begin{Bmatrix} (\varepsilon)_{s1} \\ (\varepsilon)_c \\ (\varepsilon)_{s2} \end{Bmatrix}^{\mathrm{T}} \begin{bmatrix} [D^*]_{s1} & & \\ & [D^*]_c & \\ & & [D^*]_{s2} \end{bmatrix} \begin{Bmatrix} (\varepsilon)_{s1} \\ (\varepsilon)_c \\ (\varepsilon)_{s2} \end{Bmatrix} \mathrm{d}x, \tag{14}$$

$$U_t = -b \int_0^l \begin{Bmatrix} (\varepsilon)_{s1} \\ (\varepsilon)_c \\ (\varepsilon)_{s2} \end{Bmatrix}^{\mathrm{T}} \begin{bmatrix} \left[D_1^*\right]_{s1} \\ \left[D_1^*\right]_c \\ \left[D_1^*\right]_{s2} \end{bmatrix} \mathrm{d}x. \tag{15}$$

The suffixes s_1, s_2 and c refers to the quantities corresponding to the bottom stiff layer, top stiff layer and core, respectively. The finite element formulation is similar to the Khatua and Cheung's [10] formulation and

the procedure is given as follows:

$$\begin{Bmatrix} (\varepsilon)_{s1} \\ (\varepsilon)_c \\ (\varepsilon)_{s2} \end{Bmatrix} = \begin{Bmatrix} \begin{pmatrix} \varepsilon^0_{xx} \\ k^0_{xx} \end{pmatrix}_{s1} \\ (\gamma_{xz}) \\ \begin{pmatrix} \varepsilon^0_{xx} \\ k^0_{xx} \end{pmatrix}_{s2} \end{Bmatrix} = \begin{Bmatrix} \dfrac{\partial u_1}{\partial X} \\ \dfrac{\partial^2 w}{\partial X^2} \\ \gamma_{XZ} \\ \dfrac{\partial u_2}{\partial X} \\ \dfrac{\partial^2 w}{\partial X^2} \end{Bmatrix} = [B]\{\delta\}; \quad \{\delta\} = \begin{Bmatrix} u_1^1 \\ u_2^1 \\ w^1 \\ \theta^1 \\ u_1^2 \\ u_2^2 \\ w^2 \\ \theta^2 \end{Bmatrix}, \tag{16}$$

where $[B]$ is the strain-displacement matrix, same as given by Khatua and Cheung [10] and $\{\delta\}$ is a vector of elemental nodal displacements. The Eq. (16) is substituted in the Eqs. (14) and (15) and minimization of total potential with respect to nodal displacements $\{\delta\}$, which gives the following finite element equation:

$$[K]\ \{\delta\} = \{F_t\}, \tag{17}$$

$$[K] = [K]_R + [K]_I,$$

where $[K]$ is the stiffness matrix which consists of the real $[K]_R$ and the imaginary part $[K]_I$ due to the complex shear modulus of viscoelastic core, and $\{F_t\}$ is the thermal load vector which is defined as follows:

$$[K] = b\int_0^l [B]^{\mathrm{T}}[D][B]\,\mathrm{d}x, \tag{18}$$

$$[F_t] = b\int_0^l [B]^{\mathrm{T}}[D_1]\,\mathrm{d}x, \tag{19}$$

where

$$[D] = \begin{bmatrix} [D^*]_{s1} & & \\ & [D^*]_c & \\ & & [D^*]_{s2} \end{bmatrix} \quad [D_1] = \begin{bmatrix} [D_1^*]_{s1} \\ [D_1^*]_c \\ [D_1^*]_{s2} \end{bmatrix}.$$

2.2. Geometric stiffness matrix

The geometric stiffness matrix is derived as follows. For a sandwich beam, the work done by membrane initial stresses during large transverse displacements is given by

$$[U_g] = \frac{1}{2}b\int_0^l \left((N_x^0)_{s1}(N_x^0)_{s2}\right) \begin{pmatrix} \left(\dfrac{\partial w}{\partial x}\right)_1^2 \\ \left(\dfrac{\partial w}{\partial x}\right)_2^2 \end{pmatrix} \mathrm{d}x, \tag{20}$$

where $[U_g]$ is the strain energy, $(N_x^0)_{si}$ and $(\partial w/\partial x)_i^2$ are initial stress resultants and nonlinear strains, $i = 1$ and 2 for top and bottom stiff layers, respectively.

The above Eq. (20) can be written as

$$[U_g] = \frac{1}{2} b \int_0^l \begin{pmatrix} \left(\frac{\partial w}{\partial x}\right)_1 \\ \left(\frac{\partial w}{\partial x}\right)_2 \end{pmatrix}^{\mathrm{T}} \begin{pmatrix} (N_x^0)_{s1} & \\ & (N_x^0)_{s2} \end{pmatrix} \begin{pmatrix} \left(\frac{\partial w}{\partial x}\right)_1 \\ \left(\frac{\partial w}{\partial x}\right)_2 \end{pmatrix} \mathrm{d}x, \tag{21}$$

$$\begin{pmatrix} \left(\frac{\partial w}{\partial x}\right)_1 \\ \left(\frac{\partial w}{\partial x}\right)_2 \end{pmatrix} = [B_g]\{\delta\}. \tag{22}$$

Substituting Eq. (22) in Eq. (21) we get

$$U_g = \frac{1}{2}\{\delta\}^{\mathrm{T}}[K_g]\{\delta\}, \tag{23}$$

where $[K_g]$ is called the geometric stiffness matrix given by

$$[K_g] = b \int_0^l \{B_g\}^{\mathrm{T}} [\sigma^0] \{B_g\} \, \mathrm{d}x. \tag{24}$$

2.3. Damping matrix

Damping matrix $[C]$ is evaluated using piezoelectric constitutive equations as follows. In general, a piezoelectric material responds to force or pressure and generates a charge or voltage this is called direct piezoelectric effect given by Eq. (25). On the other hand, the material exhibits stress or strain changes when a strong external charge or voltage is applied, this effect is called converse piezoelectric effect given by Eq. (26) presented in Ref. [19].

$$\{D\} = [e] \ \{S\} + [\varepsilon] \ \{E\}, \tag{25}$$

$$\{\sigma\} = [c] \ \{S\} - [e]^{\mathrm{T}} \ \{E\}, \tag{26}$$

where $\{\sigma\}$, $\{S\}$, $\{D\}$, $\{E\}$, $[e]$, $[c]$, $[\varepsilon]$ denote the stress, strain, electric displacement, electric field vectors, piezoelectric, elasticity and dielectric matrix, respectively. The direct piezoelectric effect (25) can be written for three-dimensional cases as follows [19]:

$$\begin{Bmatrix} D_1 \\ D_2 \\ D_3 \end{Bmatrix} = \begin{bmatrix} e_{11} & e_{12} & e_{13} & e_{14} & e_{15} & e_{16} \\ e_{21} & e_{22} & e_{23} & e_{24} & e_{25} & e_{26} \\ e_{31} & e_{32} & e_{33} & e_{34} & e_{35} & e_{36} \end{bmatrix} \begin{Bmatrix} S_1 \\ S_2 \\ S_3 \\ S_4 \\ S_5 \\ S_6 \end{Bmatrix} + \begin{bmatrix} \varepsilon_{11} & & \\ & \varepsilon_{22} & \\ & & \varepsilon_{33} \end{bmatrix} \begin{Bmatrix} E_1 \\ E_2 \\ E_3 \end{Bmatrix}. \tag{27}$$

According to the assumptions of beam theory, the strains in second and third directions are neglected and also it is assumed that there are no shear strains in the stiff layer. The above equation is reduced to beam as follows:

$$\begin{Bmatrix} D_1 \\ D_2 \\ D_3 \end{Bmatrix} = \begin{bmatrix} 0 & 0 & 0 & 0 & e_{15} & 0 \\ 0 & 0 & 0 & e_{24} & 0 & 0 \\ e_{31} & e_{32} & e_{33} & 0 & 0 & 0 \end{bmatrix} \begin{Bmatrix} \frac{\partial u}{\partial x} - z\frac{\partial^2 w}{\partial x^2} \\ 0 \\ 0 \\ 0 \\ 0 \\ 0 \end{Bmatrix} + \begin{bmatrix} 0 & & \\ & 0 & \\ & & \varepsilon_{33} \end{bmatrix} \begin{Bmatrix} 0 \\ 0 \\ -\frac{\overline{\phi}_s}{t_s} \end{Bmatrix}, \tag{28}$$

where $S_1 = ((\partial u/\partial x) - z(\partial^2 w/\partial x^2))$ and $E_3 = -(\overline{\phi}_s/t_s)$.

After simplification, the average sensor voltage $\overline{\phi}_s$ obtained by integrating over the area of the sensor is given by

$$\overline{\phi}_s = \frac{-t_s b}{\varepsilon_{33} A_s}\left(\int_0^x \left\{\frac{t_b + t_s}{2} e_{31} \quad e_{31} \quad 0 \quad 0 \quad 0\right\}[B]\{\delta\}\,\mathrm{d}x\right), \tag{29}$$

where $\overline{\phi}_s$, t_s, t_b, b, A_s, ε_{33}, e_{31}, $[B]$, $\{\delta\}$ are the average sensor output voltage over the surface of the sensor, thickness of the sensor, thickness of the base beam, breadth of the beam, surface area of the sensor, dielectric constant, stress electric coefficient, matrix of strain displacement and vector of nodal displacements, respectively. The actuating voltage ϕ_a according to negative feedback velocity algorithm is given by

$$\phi_a = -G\dot{\overline{\phi}}_s, \tag{30}$$

where ϕ_a, G are the actuating voltage and control gain, respectively:

$$\phi_a = \frac{G t_s b}{\varepsilon_{33} A_s}\left(\int_0^x \left\{\frac{t_b + t_s}{2} e_{31} \quad e_{31} \quad 0 \quad 0 \quad 0\right\}[B]\{\dot{\delta}\}\,\mathrm{d}x\right), \tag{31}$$

$$\phi_a = K_{u\phi S}\{\dot{\delta}\}, \tag{32}$$

where

$$K_{u\phi S} = \frac{G t_s b}{\varepsilon_{33} A_s}\int_0^x \left\{\frac{t_b + t_s}{2} e_{31} \quad e_{31} \quad 0 \quad 0 \quad 0\right\}[B]\,\mathrm{d}x.$$

Since the mechanical strains in actuator layer are negligible, then Eq. (26) reduces to

$$\{\sigma\} = -[e]^{\mathrm{T}}\ \{E\}. \tag{33}$$

The virtual work expression is given by

$$= \int_v \{S\}^{\mathrm{T}}\{\sigma\}\,\mathrm{d}v. \tag{34}$$

Substituting Eq. (33) into Eq. (34) we get

$$= -\int_v \{S\}^{\mathrm{T}}[e]^{\mathrm{T}}\{E\}\,\mathrm{d}v, \tag{35}$$

$$= -\int_v \begin{Bmatrix} \dfrac{\partial u}{\partial x} - z\dfrac{\partial^2 w}{\partial x^2} \\ 0 \\ 0 \\ 0 \\ 0 \\ 0 \end{Bmatrix}^{\mathrm{T}} \begin{bmatrix} 0 & 0 & 0 & 0 & e_{15} & 0 \\ 0 & 0 & 0 & e_{24} & 0 & 0 \\ e_{31} & e_{32} & e_{33} & 0 & 0 & 0 \end{bmatrix}^{\mathrm{T}} \begin{Bmatrix} 0 \\ 0 \\ -\dfrac{\phi_a}{t_a} \end{Bmatrix} \mathrm{d}v. \tag{36}$$

After simplification, the elemental damping matrix $[C]$ is given by

$$[C] = \left[b\int_0^x [B]^{\mathrm{T}}\left\{0 \quad 0 \quad 0 \quad 0 \quad e_{31}\right\}^{\mathrm{T}}\mathrm{d}x\right]K_{u\phi S}. \tag{37}$$

2.4. Evaluation of loss factor and frequency

The combined composite and viscoelastic (C + V) damping loss factor for nth mode at atmospheric temperature can be calculated by

$$\eta_n = \frac{\phi_n^{\mathrm{T}}[K]_I\phi_n}{\phi_n^{\mathrm{T}}[K]_R\phi_n}, \tag{38}$$

where $[K]_R$ and $[K]_I$ are the real and imaginary parts of the stiffness matrices $[K]$, respectively, and ϕ_n is nth mode eigenvector.

The following eigenvalue problem has to be solved to get the natural frequencies under thermal environment:

$$\left[[K]+[K]_g\right]-\omega^2[M]=0, \tag{39}$$

where ω is the natural frequency.

The combined composite and viscoelastic (C + V) damping loss factor for a given temperature can be calculated by

$$\eta_n=\frac{\phi_n^{\mathrm{T}}(K)_I\phi_n}{\phi_n^{\mathrm{T}}\left((K)_R+(K)_g\right)\phi_n}. \tag{40}$$

For obtaining the active loss factor, the following eigenvalue problem is solved:

$$\begin{bmatrix}-[C] & -[M]\\ [0] & [M]\end{bmatrix}\begin{Bmatrix}\{\dot{\delta}_G\}\\ \{\ddot{\delta}_G\}\end{Bmatrix}=\lambda\begin{bmatrix}[K]+[K_g] & [0]\\ [0] & [M]\end{bmatrix}\begin{Bmatrix}\{\delta_G\}\\ \{\dot{\delta}_G\}\end{Bmatrix}, \tag{41}$$

where the eigenvalues λ are complex conjugates and are given by $\lambda=\lambda_{Rn}\pm i\lambda_{In}$ whose imaginary values give natural frequencies. The nth modal active loss factor is given by

$$\eta_{an}=\frac{-\lambda_{Rn}}{\sqrt{\lambda_{Rn}^2+\lambda_{In}^2}}.$$

Table 2
Comparison of frequency and loss factor at different modes

Mode no.	Frequency		Loss factor	
	Present	Ref. [14]	Present	Ref. [14]
1	227.91	228.95	0.057	0.058
2	639.99	642.90	0.155	0.158
3	1287.05	1292.81	0.267	0.276
4	2199.89	2209.52	0.241	0.250

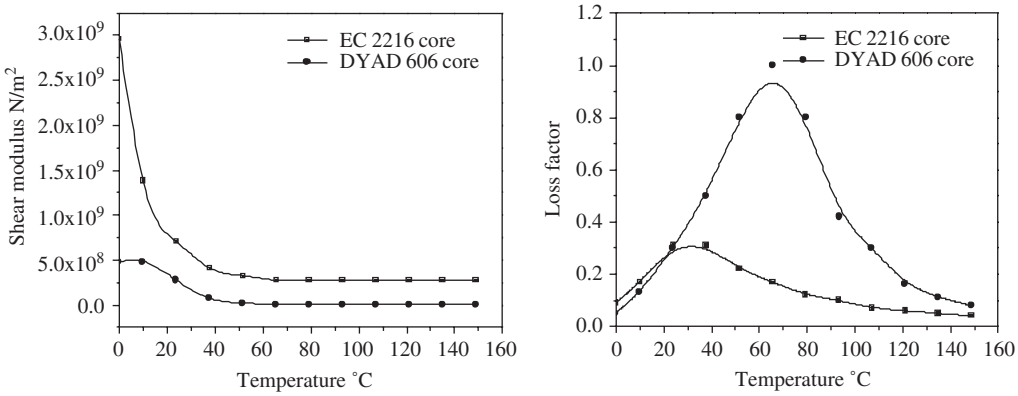

Fig. 2. Viscoelastic properties of EC2216 and DYAD606 core material [16].

The total loss factor for the nth mode is the sum of composite, viscoelastic and active loss factors of the nth mode given by

$$\eta_{Tn} = \eta_n + \eta_{an}. \tag{42}$$

3. Results and discussion

To establish the hybrid damping, a closed loop feed back system with feed back gain 0.01 is used in the present study. The results obtained by the present study for isotropic ACLD beam under room temperature are compared with those reported by Pradeep and Ganesan [14]. The frequencies and loss factor at different modes have a good agreement with the results presented in Ref. [14] as shown in Table 2.

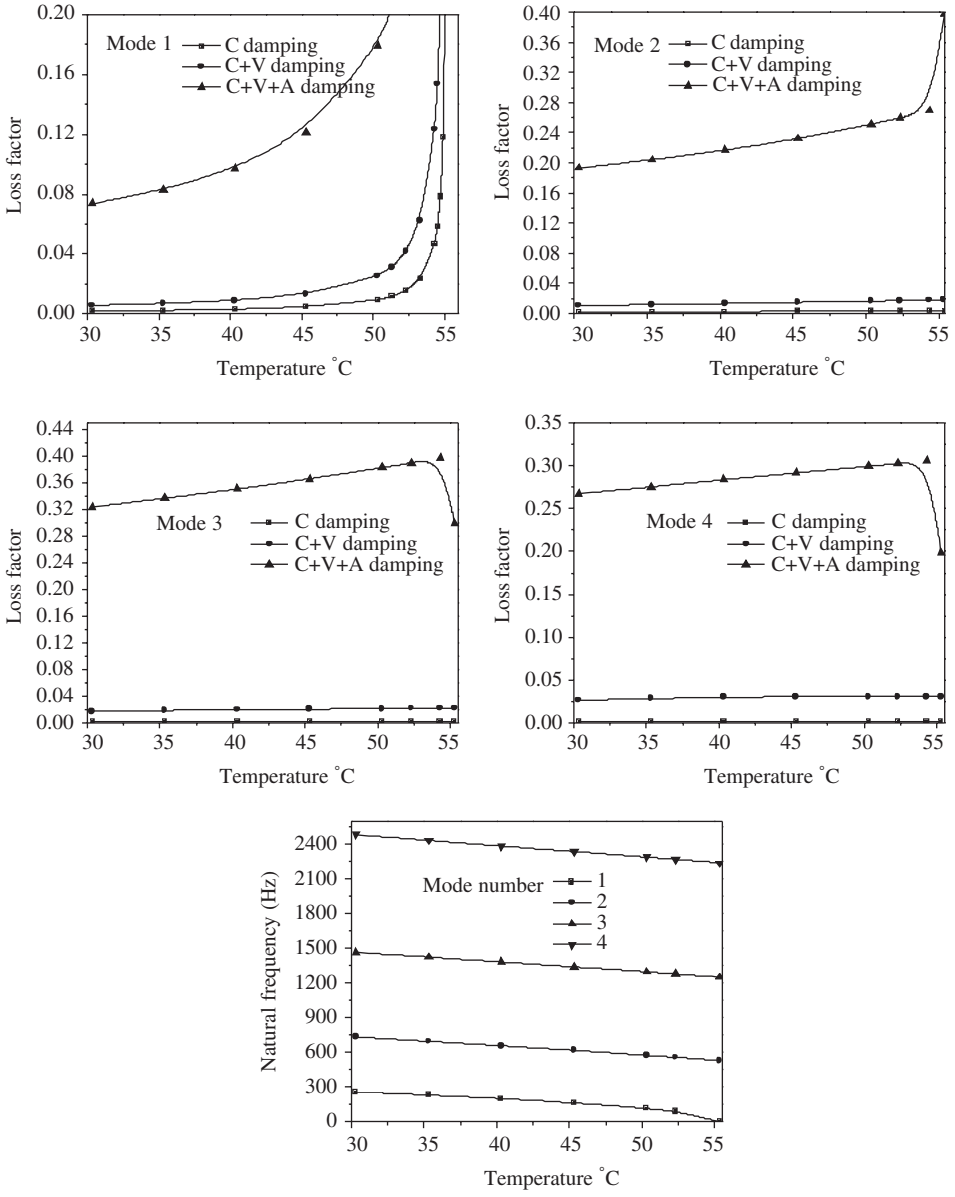

Fig. 3. Loss factor and frequency with tip temperature for a beam with EC2216 as core, $t_c = 0.25$ mm.

3.1. Beam with fixed–fixed (F–F) boundary condition

In order to understand the different types of damping present in the system, the study has been carried out for the following cases:

Case 1: Structural damping of composite alone (*C*) accounted for the study.

Case 2: Composite and viscoelastic (C + V) damping accounted for the study.

Case 3: Composite, viscoelastic and active (C + V + A) damping accounted for the study.

Composite damping is the property of the material obtained from the experiment. The composite and viscoelastic loss factor under thermal environment are evaluated by Eq. (40), which uses modal strain energy method, and the total damping is calculated by Eq. (42), which uses the state space approach. The present study is carried out for different core materials and core thickness by considering the complex shear modulus

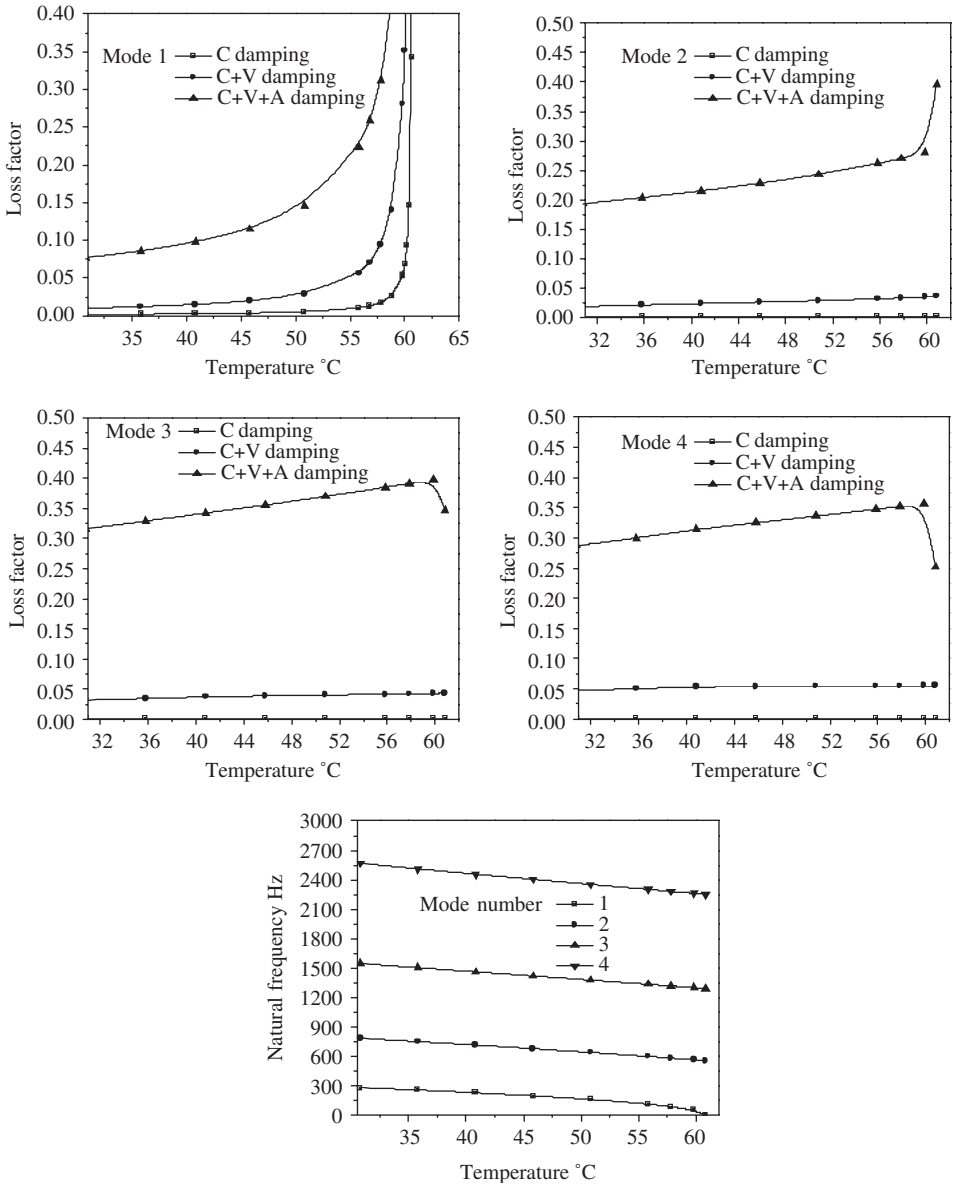

Fig. 4. Loss factor and frequency with tip temperature for a beam with EC2216 as core, $3t_c = 0.75$ mm.

of the core. The variation of shear modulus and loss factor with temperature for two types of cores is given by Nashif et al. [16] as shown in Fig. 2.

3.1.1. Effect of temperature on frequency and loss factor for different core thickness and core material

To start with, the study has been carried out for zero fiber angle with damping material EC2216. The variation of natural frequency and loss factor with temperature is shown in Fig. 3 for core thickness 0.25 mm. It is seen from Fig. 3 that the composite damping and combined composite and viscoelastic damping increases with temperature for all the modes. The first and second mode shows that the total damping factor increases with temperature. For the higher modes, the total damping reaches a maximum value and falls down. This behavior imitates the variation of material loss factor with temperature as given in Ref. [16] shown in Fig. 2.

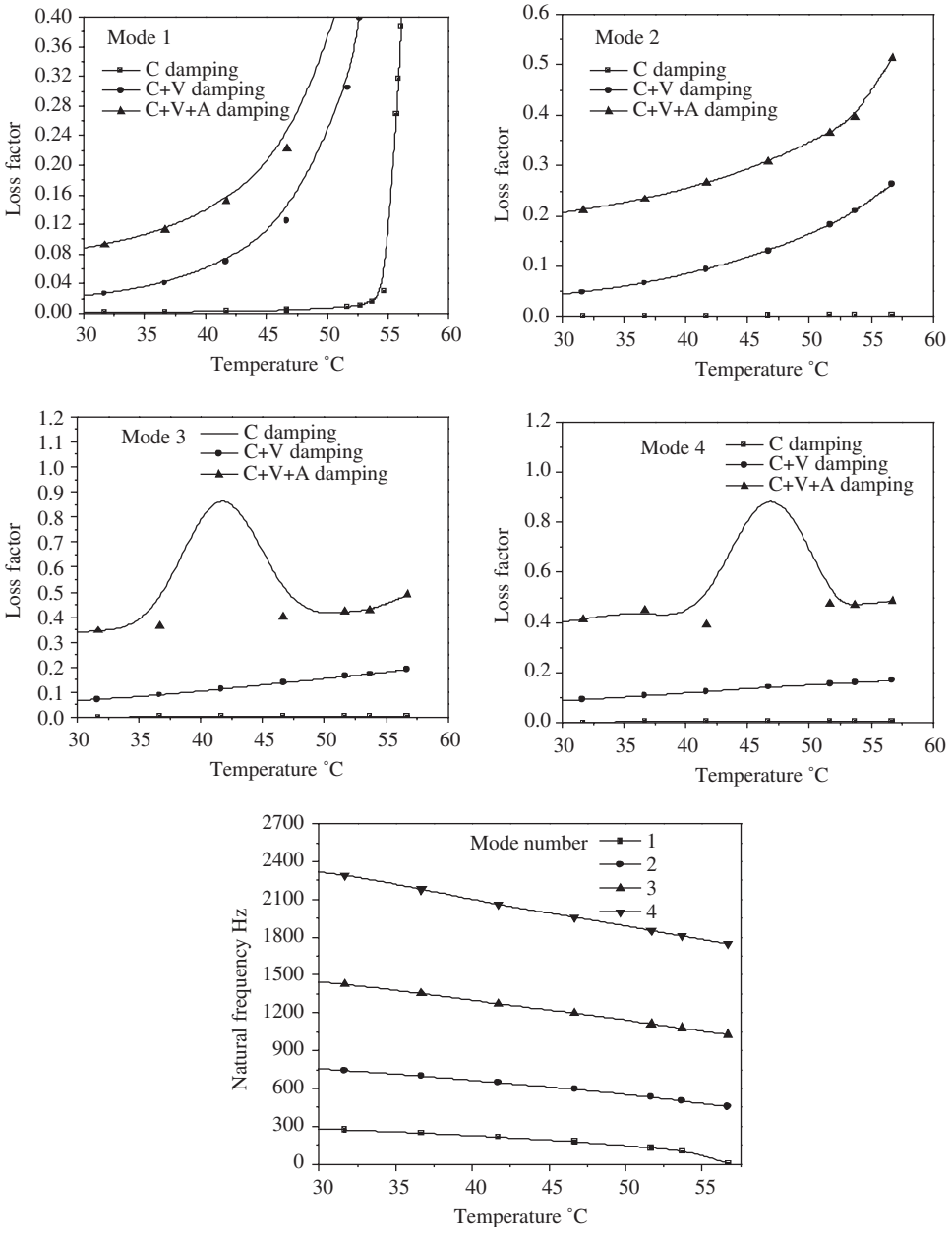

Fig. 5. Loss factor and frequency with tip temperature for a beam with DYAD606 as core, $3t_c = 0.75$ mm.

The influence of geometric stiffness matrix is felt on the first and second mode and hence the damping goes on increasing as the denominator of Eq. (40) decreases. In case of higher modes, the buckling temperature is much higher and the material property of viscoelastic core dominates and hence the damping follows the variation pattern similar to that given in Ref. [16] shown in Fig. 2. The frequency is found by solving the eigenvalue problem given by Eq. (39). When the temperature approaches the buckling temperature, the frequency tends to zero and loss factor value shoots up as shown in Fig. 3. The active damping in the system increases with temperature for first two modes. The contribution of active damping to the total damping (C + V + A damping) is much higher compared to other two types of damping. The dominant mechanism of damping is active damping.

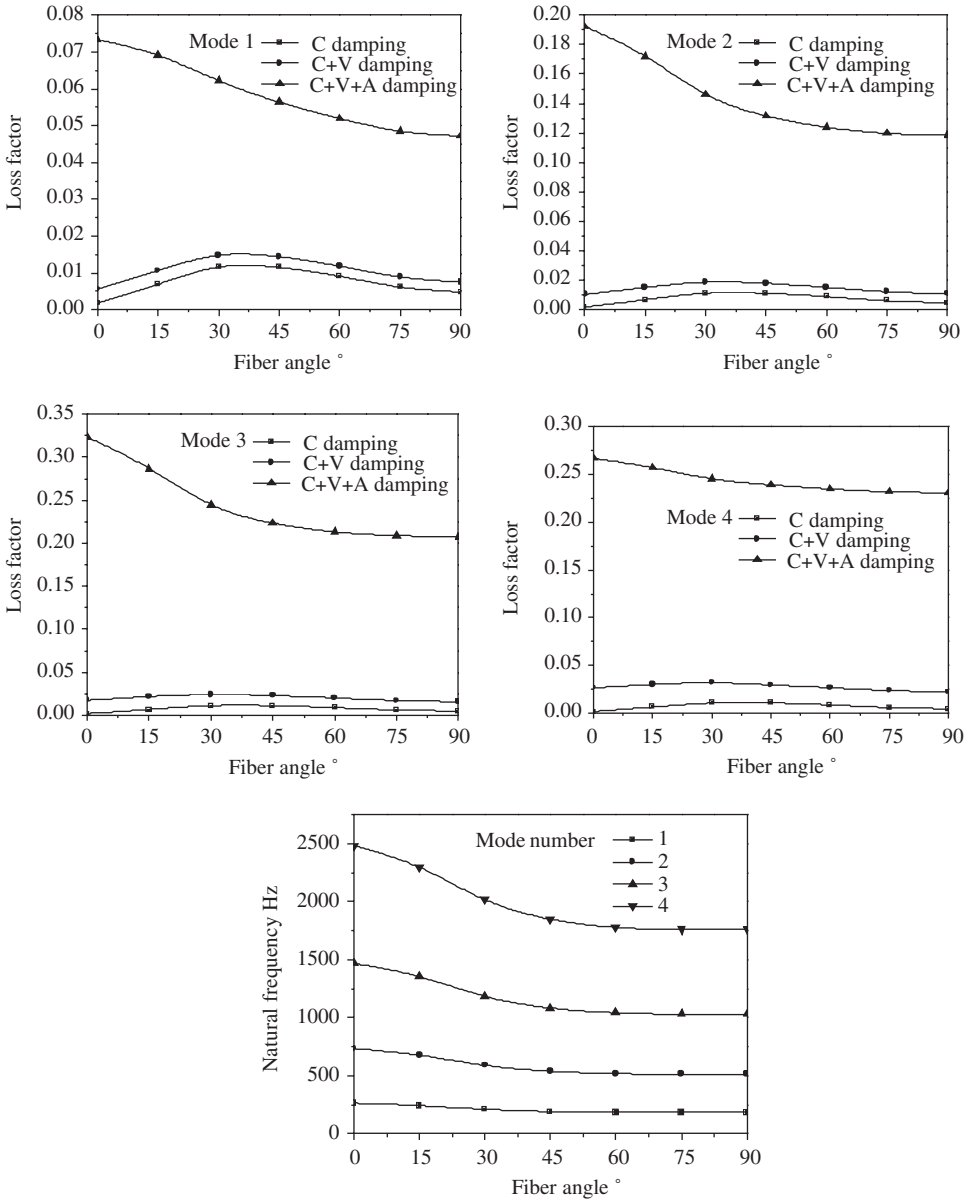

Fig. 6. Loss factor and frequency with fiber angle for a beam with EC2216 as core, $t_c = 0.25$ mm.

3.1.1.1. Influence of core thickness. Figs. 3 and 4 shows the variation of frequency and damping for EC2216 core with thickness 0.25 and 0.75 mm, respectively, at zero fiber angle. It is seen from the figures that as the core thickness increases viscoelastic damping in the beam increases. The buckling temperature increases slightly with an increase in the core thickness as expected. The natural frequency increases with core thickness, because increase in core thickness leads to increase in the stiffness of the structure.

3.1.1.2. Influence of core material. Figs. 4 and 5 show the variation of loss factor and frequency with temperature using EC2216 and DYAD606 core material, respectively, at zero fiber angle. The comparison of Figs. 4 and 5 shows that core material play a very important role in total damping of the beam. For the beam, composite damping has no appreciable effect in both the cases. The combination of composite and viscoelastic

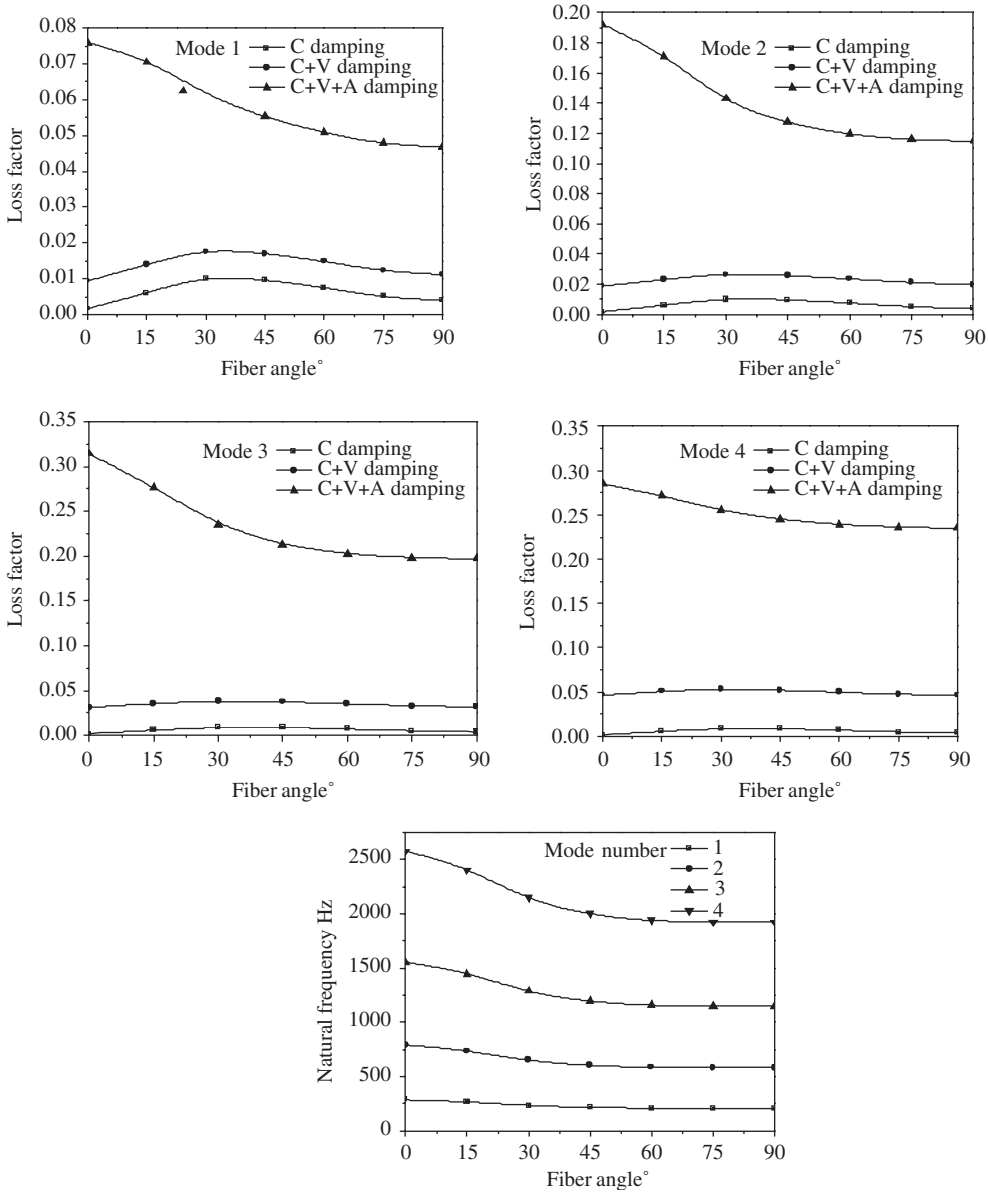

Fig. 7. Loss factor and frequency with fiber angle for a beam with EC2216 as core, $3t_c = 0.75$ mm.

damping of DYAD606 core material is more for all temperatures and all modes compared to EC2216 core. The viscoelastic damping of DYAD606 core is more at all temperatures because of the sudden fall in the shear modulus at all temperatures compared to EC2216 core material shown in Fig. 2. Total loss factor increases with increase in temperature for all modes in case of DYAD606 compared to EC2216 shown in Figs. 5 and 4, respectively. The buckling temperature and natural frequency of the beam with DYAD606 core is lower than that of EC2216 core which is due to the lower modulus of DYAD606 core shown in Fig. 2.

3.1.2. Effect of fiber angle on frequency and loss factor for different core thickness and core material

Fig. 6 shows the variation of natural frequency and loss factor for different fiber orientations of the composite beam with EC2216 core at room temperature. The composite and viscoelastic damping are

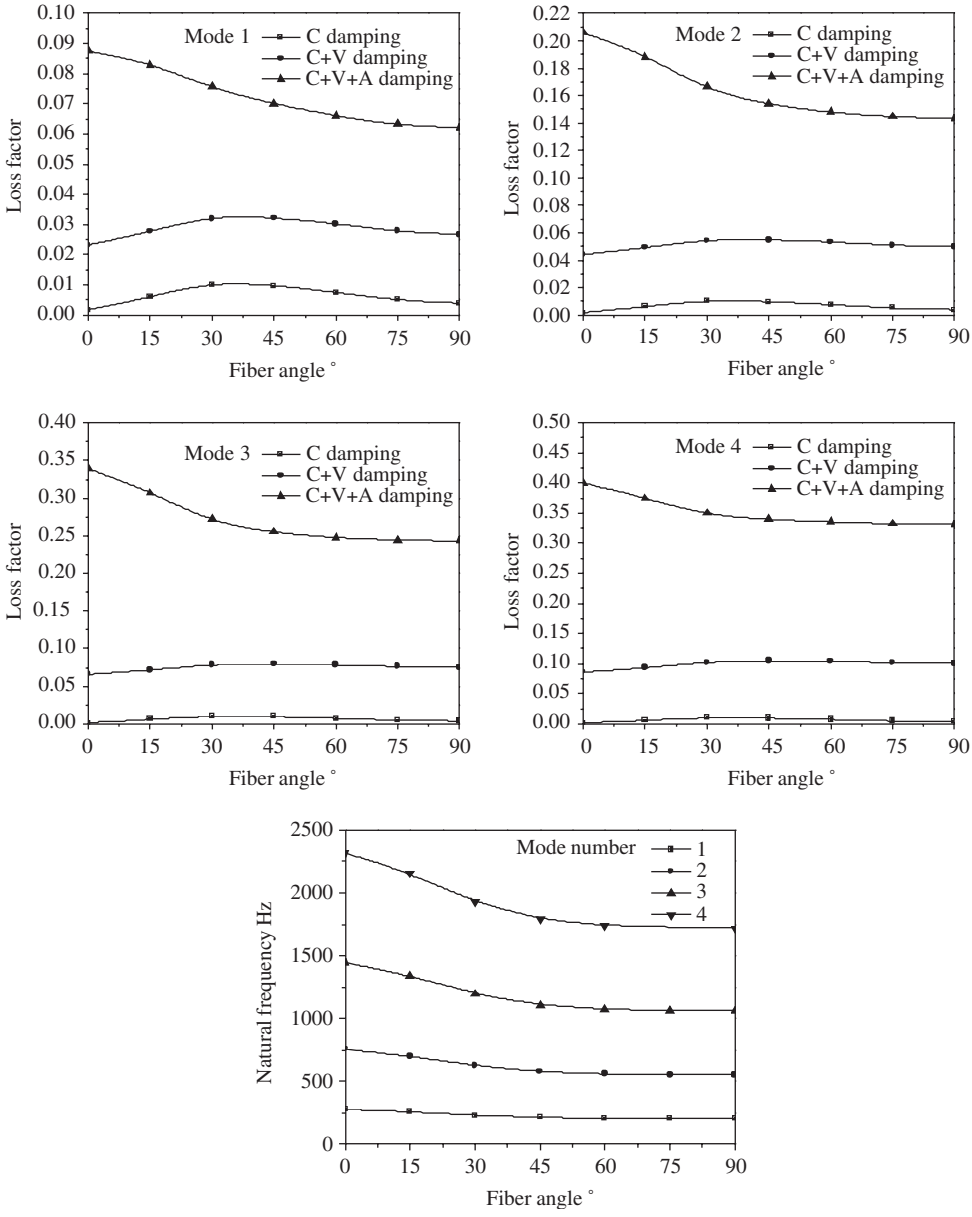

Fig. 8. Loss factor and frequency with fiber angle for a beam with DYAD 606 as core, $3t_c = 0.75$ mm.

calculated by Eq. (38). The natural frequency decreases with an increase in the fiber angle from 0° to 90°. At higher modes, there is maximum reduction in frequency with fiber orientation compared to the fundamental mode. It is clearly observed from the figure that for the fundamental mode, the composite damping increases with the increase in the fiber angle from 0° to 45° and then onwards decreases. The combined composite and viscoelastic damping curve follows the same pattern of composite damping curve. This is because of composites having inherent damping, which is relatively higher than conventional isotropic materials. Hence, addition of viscoelastic damping may not play an important role. It is clear from the graph that the influence of active damping dominates in all modes. The total loss factor decreases with an increase in the fiber angle.

3.1.2.1. Influence of core thickness. Figs. 6 and 7 show the variation of frequency and loss factor for the EC2216 core thickness 0.25 and 0.75 mm, respectively. On increasing the core thickness of the beam, the

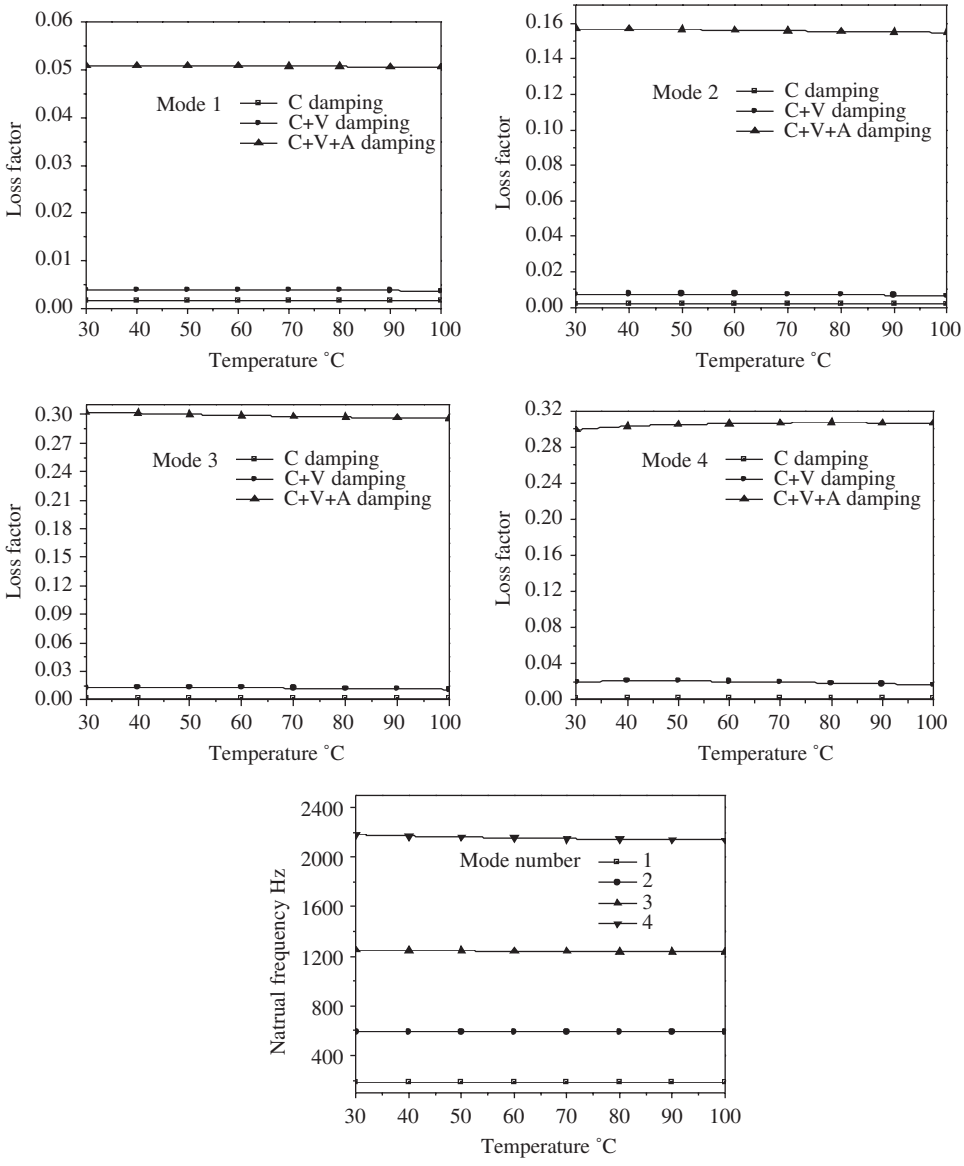

Fig. 9. Loss factor and frequency with tip temperature for a beam with EC2216 as core, $t_c = 0.25$ mm.

frequency increases for all modes because the structure becomes stiffer. Viscoelastic damping increases by increasing the core thickness of the beam for all modes. The total loss factor increases in all the modes due to the effect of viscoelastic damping shown in Figs. 6 and 7.

3.1.2.2. Effect of core material. Figs. 7 and 8 show the variation of loss factor and frequency with fiber orientation for the core materials EC2216 and DYAD606, respectively. The frequency of DYAD606 core decreases for all modes compared to EC2216 core. The core material plays an important role in viscoelastic damping. The viscoelastic damping for the DYAD606 core is considerably more for all modes compared to EC2216 core. The total damping of the structure with DYAD606 as core material increases for modes when compared with EC2216 core material. This behavior can be attributed to fall in the shear modulus of DYAD606 core material compared to EC2216.

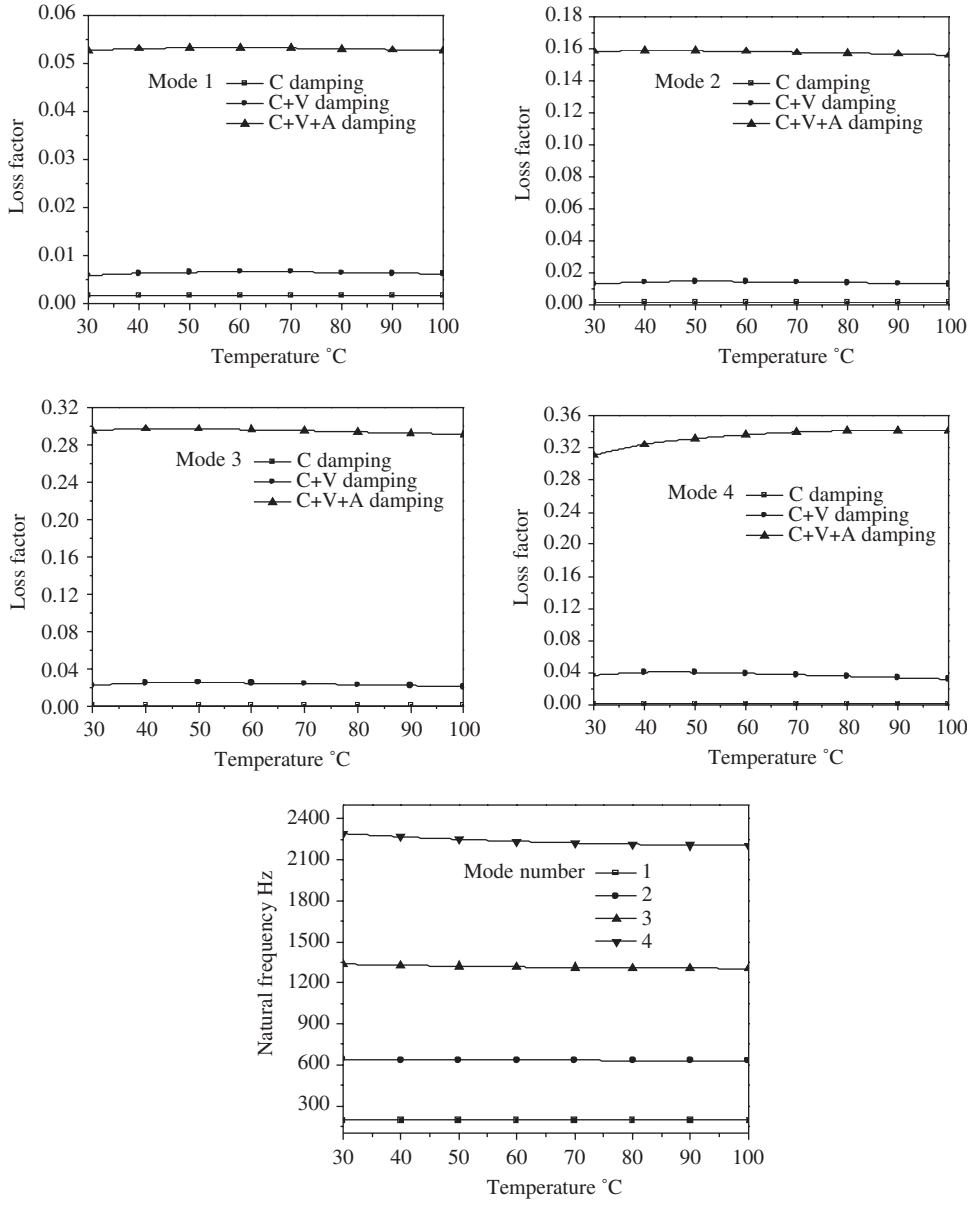

Fig. 10. Loss factor and frequency with tip temperature for a beam with EC2216 as core, $3t_c = 0.75$ mm.

3.2. Beam with fixed–simply supported (F–S) boundary condition

3.2.1. Effect of temperature on frequency and loss factor for different core thickness and core material

Fig. 9 shows the variation of frequency and damping with temperature for fixed–simply supported boundary condition at zero fiber angle. For the temperature range considered, the frequency and damping remains constant with increase in temperature. This may be expected because fixed–simply supported beams in general have very high bucking temperature. The present analysis is carried out for a lower temperature range because the viscoelastic material cannot withstand higher temperatures. Comparing Figs. 3 and 9, the natural frequency of fixed–simply supported beam is lower than the fixed–fixed beam at atmospheric temperature. The buckling temperature of fixed–fixed beam is lower than the fixed–simply supported beam. This is due to the

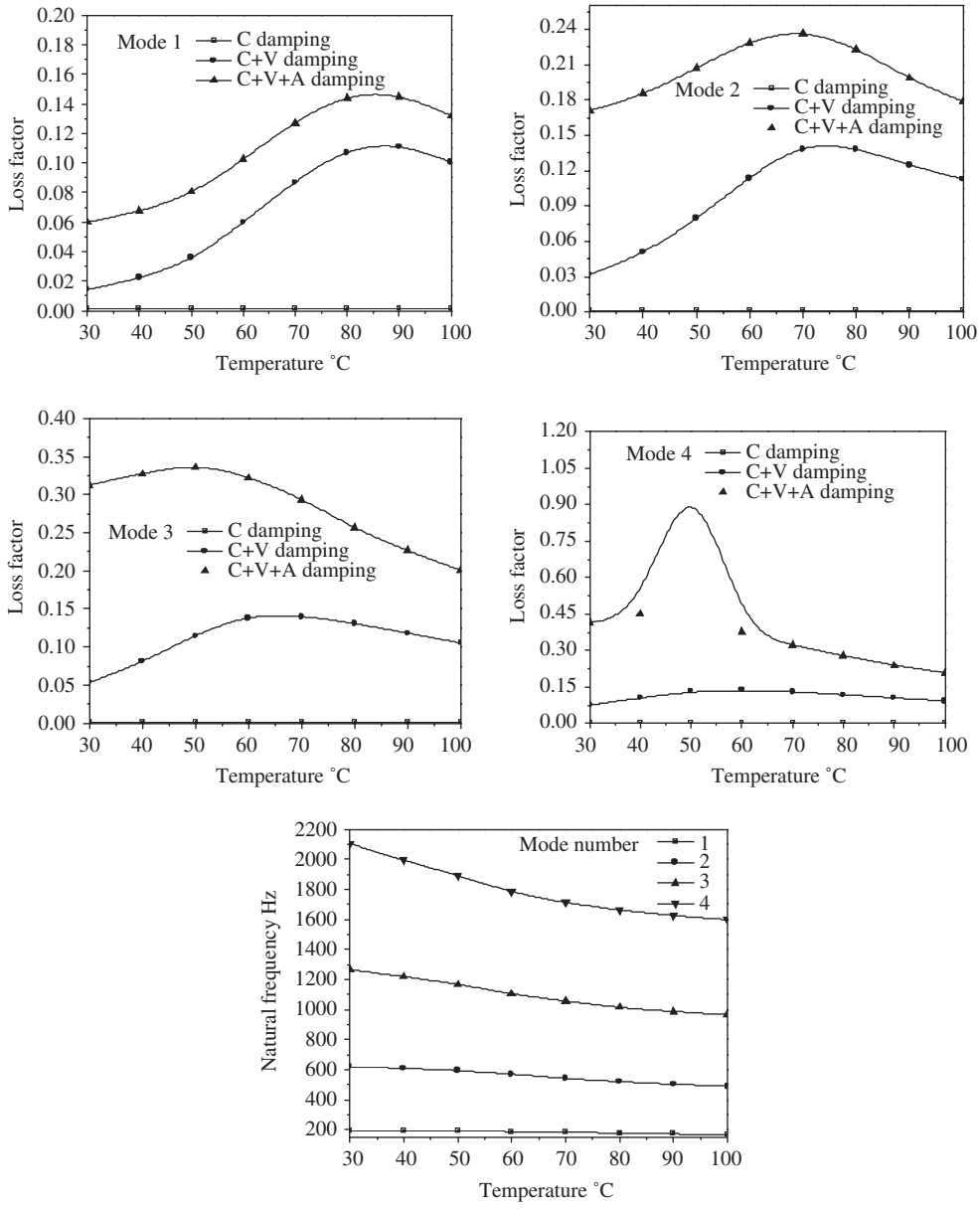

Fig. 11. Loss factor and frequency with tip temperature for a beam with DYAD606 as core, $3t_c = 0.75$ mm.

fact that the thermal stresses developed in fixed–fixed beam are very high compared to fixed–simply-supported beam.

Figs. 9 and 10 show the variation of frequency and loss factor with core thickness 0.25 and 0.75 mm, respectively. As the core thickness increases, natural frequency increases slightly and viscoelastic damping increases for all the modes. Figs. 10 and 11 show the variation of frequency and loss factor with temperature using EC22216 core and DYAD606 core materials, respectively. The frequency of beam with DYAD606 core decreases with the increase in the temperature compared to EC2216 because of lower modulus of DYAD606 core compared to EC2216 core. The viscoelastic damping of the beam with DYAD606 core increases with an increase in temperature for certain limits, then onwards it decreases, because the shear modulus of DYAD606

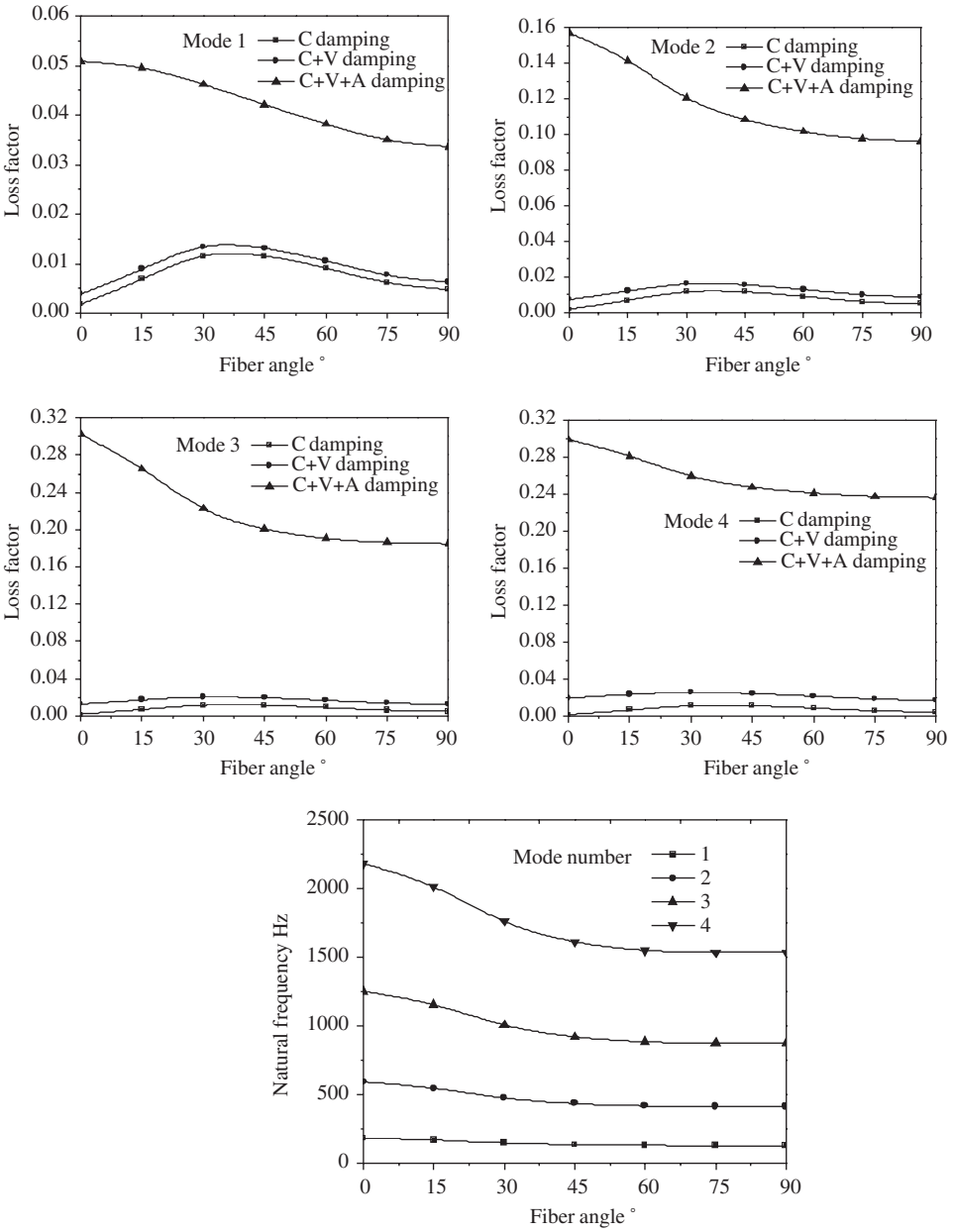

Fig. 12. Loss factor and frequency with fiber angle for a beam with EC2216 as core, $t_c = 0.25$ mm.

material decreases suddenly with temperature compared with EC2216 given in Ref. [16] as shown in Fig. 2, due to which the denominator of the expression (40) decreases and viscoelastic loss factor increases.

3.2.2. Effect of fiber angle on frequency and loss factor for different core thickness and core material

Fig. 12 shows the variation of frequency and damping with fiber angle for fixed–simply supported beam. Comparing the Figs. 6 and 12, frequency and loss factor of fixed–simply supported beam at fundamental mode is less than the fixed–fixed beam. Figs. 12 and 13 show the variation of frequency and damping with fiber angle for core thickness 0.25 and 0.75 mm at atmospheric temperature, respectively. Frequency and damping increases with an increase in the core thickness, the reason for this being the same as discussed in the foregoing Section 3.1.2.1. Fig. 14 shows the variation of frequency and loss factor with DYAD606 as core material. Comparing Figs. 13 and 14, frequency of the beam of the DYAD606 core has a slightly lower natural frequency

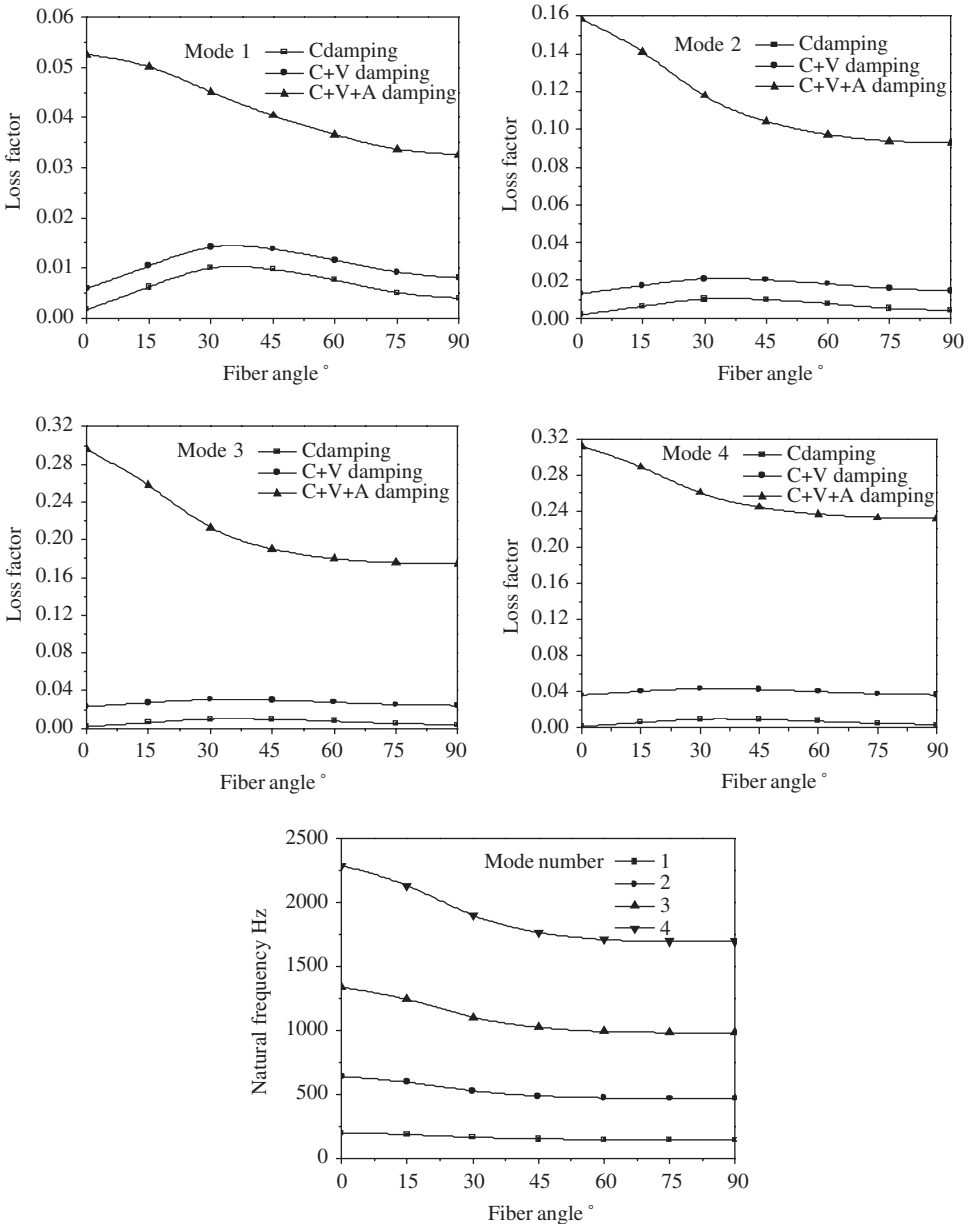

Fig. 13. Loss factor and frequency with fiber angle for a beam with EC2216 as core, $3t_c = 0.75$ mm.

than the EC2216 core. Viscoelastic damping of DYAD606 core material has a higher value compared to the EC2216 core, the explanation for this being the same as discussed in Section 3.1.2.2. Comparing Figs. 8 and 14, the frequency and total loss factor of fixed–simply supported beam is lower than the fixed–fixed beam.

4. Conclusions

In the present study, for the first time in the literature, dynamic analysis of ACLD composite beam under thermal environment is investigated. Frequency and damping variations with respect to temperature as well as fiber angle are carried out for two different boundary conditions (F–F, F–S).

1. Buckling temperature for fixed–fixed boundary conditions is very low compared to fixed–simply supported boundary conditions.

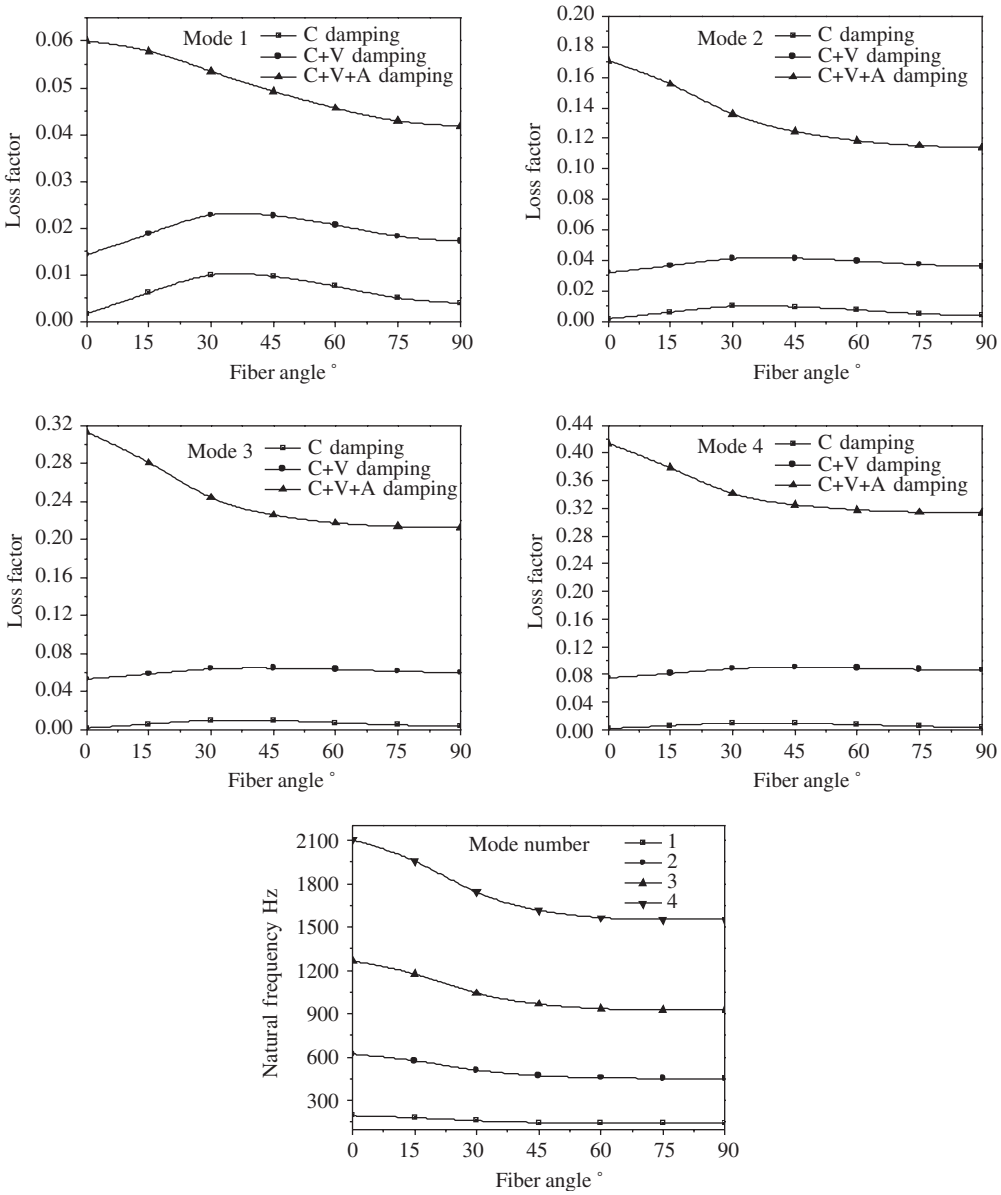

Fig. 14. Loss factor and frequency with fiber angle for a beam with DYAD606 as core, $3t_c = 0.75$ mm.

2. Increasing the core thickness, viscoelastic damping increases and also buckling temperature increases slightly.
3. Effect of core material considerably affects the thermal buckling temperature and vibration behavior.
4. Near the buckling temperature the frequency attains to zero for the first mode, and the loss factor increases tremendously.
5. The frequency and damping decreases with an increase in the fiber angle. The change of natural frequency and damping is more at higher modes compare to that of fundamental modes.
6. The combined composite and viscoelastic damping does not have much influence on the total damping; the active damping is the predominant mechanism of damping.

References

[1] M.C. Ray, J.N. Reddy, Optimal control of thin circular cylindrical laminated composite shells using active constrained layer damping treatment, *Smart Materials and Structures* 13 (2004) 64–72.

[2] M.C. Ray, J.N. Reddy, Active control of laminated cylindrical shells using piezoelectric fiber reinforced composites, *Composites Science and Technology* 65 (2005) 1226–1236.

[3] M.C. Ray, N. Mallik, Active control of laminated composite beams using a piezoelectric fiber reinforced composite layer, *Smart Materials and Structures* 13 (2004) 146–152.

[4] M.C. Ray, N. Mallik, Performance of smart damping treatment using piezoelectric fiber-reinforced composites, *AIAA Journal* 43 (1) (2005) 184–193.

[5] M.C. Ray, A. Baz, Optimization of energy dissipation of active constrained layer damping treatments of plates, *Journal of Sound and Vibration* 208 (3) (1997) 391–406.

[6] M.C. Ray, J. Oh, A. Baz, Active constrained layer damping of thin cylindrical shells, *Journal of Sound and Vibration.* 240 (5) (2001) 921–935.

[7] C. Chantalakhana, R. Stanway, Active constrained layer damping of clamped–clamped plate vibrations, *Journal of Sound and Vibration* 241 (5) (2001) 755–777.

[8] S. Yi, K.Y. Sze, A finite element formulation for composite laminates with smart constrained layer damping, *Advances in Engineering Software* 31 (2000) 529–537.

[9] B. Sun, D. Huang, Vibration suppression of laminated composite beams with a piezo-electric damping layer, *Composite Structures* 53 (2001) 437–447.

[10] T.P. Khatua, Y.K. Cheung, Bending and vibration of sandwich beams and plates, *International Journal of Numerical Methods in Engineering* 6 (1973) 11–24.

[11] P. Gaudenzi, R. Carbonaro, R. Barboni, Vibration control of an active laminated beam, *Composite Structures* 38 (1–4) (1997) 413–420.

[12] V. Balamurugan, S. Narayanan, Finite element formulation and active vibration control study on beams using smart constrained layer damping (SCLD) treatment, *Journal of Sound and Vibration* 249 (2) (2002) 227–250.

[13] L.C. Hau, E.H.K. Fung, Effect of ACLD treatment configuration on damping performance of a flexible beam, *Journal of Sound and Vibration* 269 (2004) 549–567.

[14] V. Pradeep, N. Ganesan, Vibration behaviour of ACLD treated beams under thermal environment, *Journal of Sound and Vibration* 292 (2006) 1036–1045.

[15] J.-S. Chang, J.-W. Shyong, Thermally induced vibration of laminated circular cylindrical shell panels, *Composites Science and Technology* 51 (1994) 419–427.

[16] A.D. Nashif, D.I.G. Jones, J.P. Henderson, *Vibration Damping*, first ed., Wiley, New York, 1985.

[17] V. Pradeep, N. Ganesan, Buckling and vibration of sandwich beams with viscoelastic core under thermal environment, *Journal of Sound and Vibration* 286 (4) (2005) 1067–1074.

[18] W.J. Chen, P.D. Lin, L.W. Chen, Thermal buckling behavior of thick composite laminated plates under non uniform temperature distribution, *Computers and Structures* 41 (4) (1991) 637–645.

[19] H.S. Tzou, Y. Bao, A theory on anisotropic piezothermoelastic shell laminates with sensor/actuator applications, *Journal of Sound and Vibration* 184 (3) (1995) 453–473.